Role of vascular endothelial growth factor signaling in *Schistosoma*-induced experimental pulmonary hypertension

Jacob J. Chabon,[1] Liya Gebreab,[1] Rahul Kumar,[1] Elias Debella,[1] Takeshi Tanaka,[1] Dan Koyanagi,[1] Alexandra Rodriguez Garcia,[1] Linda Sanders,[1] Mario Perez,[1] Rubin M. Tuder,[1,2] Brian B. Graham[1,2]

[1]Division of Pulmonary Sciences and Critical Care Medicine, Department of Medicine, Anschutz Medical Campus, University of Colorado Denver, Aurora, Colorado, USA; [2]Pulmonary Vascular Research Institute

Abstract: There is significant evidence that Th2 (T helper 2)-mediated inflammation supports the pathogenesis of both human and experimental animal models of pulmonary hypertension (PH). A key immune regulator is vascular endothelial growth factor (VEGF), which is produced by Th2 inflammation and can itself contribute to Th2 pulmonary responses. In this study, we interrogated the role of VEGF signaling in a murine model of schistosomiasis-induced PH with a phenotype of significant intrapulmonary Th2 inflammation, vascular remodeling, and elevated right ventricular pressures. We found that VEGF receptor blockade partially suppressed the levels of the Th2 inflammatory cytokines interleukin (IL)-4 and IL-13 in both the lung and the liver after *Schistosoma mansoni* exposure and suppressed pulmonary vascular remodeling. These findings suggest that VEGF positively contributes to schistosomiasis-induced vascular inflammation and remodeling, and they also provide evidence for a VEGF-dependent signaling pathway necessary for pulmonary vascular remodeling and inflammation in this model.

Keywords: pulmonary hypertension, inflammation, VEGF, schistosomiasis.

Pulm Circ 2014;4(2):289-299. DOI: 10.1086/675992.

INTRODUCTION

Despite significant evidence suggesting a role for inflammation in the development of pulmonary hypertension (PH), documentation of a causal role for inflammation in the disease is largely lacking.[1-4] Potentially suppressed interleukin (IL)-13 signaling has been reported in the lungs of humans with idiopathic pulmonary arterial hypertension (PAH), mice with hypoxia-induced PH, and rats with monocrotaline-induced PH.[5] Alternatively, induction of an adaptive T helper 2 (Th2) immune response in the lungs of mice suffices to cause pulmonary arterial muscularization, while depletion of the Th2 inflammatory cytokine IL-13 significantly attenuates such remodeling.[6] A key immune regulator candidate is vascular endothelial growth factor (VEGF), which can enhance Th2-mediated inflammation and has also been shown to play a critical role in the development of Th2-induced bronchial vascular remodeling.[7,8] IL-13 can, in turn, increase VEGF production,[9] potentially forming a proinflammatory feed-forward loop.

In contrast to the concept of VEGF inducing inflammation and pulmonary vascular disease in mouse models, pharmacological VEGF receptor (VEGFR) blockade (typically with SU5416 treatment), coupled with chronic hypoxia, results in severe angio-obliterative experimental PH in the rat.[10] Recent evidence indicates that exogenous Th2 inflammation (caused by ovalbumin inhalation) also synergizes with VEGFR blockade to result in severe PH in the rat.[11] However, mice comparably immunized with ova and treated with SU5416 do not develop PH,[12] suggesting differential roles for VEGFR-mediated signaling, in the context of a Th2 inflammatory response, in the mouse compared to the rat.

We have established a mouse model of schistosomiasis-induced PH in which intraperitoneal sensitization with *Schistosoma mansoni* ova followed by intravenous augmentation with ova results in significant intrapulmonary Th2 inflammation coupled with pulmonary vascular remodeling and ele-

Address correspondence to Dr. Brian B. Graham, Program in Translational Lung Research, Division of Pulmonary Sciences and Critical Care Medicine, University of Colorado Denver, Research 2, 9th floor, Mail Stop C-272, 12700 East 19th Avenue, Aurora, CO 80045, USA. E-mail: brian.graham@ucdenver.edu.

Submitted January 14, 2014; Accepted February 4, 2014; Electronically published May 20, 2014.

vated right ventricular pressures.[13-15] The role of inflammation in the development of PH in this model is demonstrated by the absence of PH after intravenous eggs alone are administered, without allowing an augmented adaptive immune response following intraperitoneal sensitization.[13] In contrast to other experimental models of pulmonary Th2 vascular responses, this model is highly relevant to the human disease of schistosomiasis-associated PAH caused by chronic infection with the trematode *S. mansoni*, the third-most-prevalent parasitic infection worldwide, which affects more than 200 million people and is one of the most common causes of WHO Group 1 PAH worldwide.[16-20] In addition, this model provides an ideal setting in which to further investigate potentially differential roles of VEGF signaling in the context of pulmonary Th2-mediated inflammation in the mouse. VEGF may also regulate vascular disease through Rho kinase signaling[21] and could interact with *Schistosoma* exposure in this regard, as we have previously observed a significant component of Rho kinase–mediated vasoconstriction in *Schistosoma*-induced PH.[14]

We thus hypothesized that VEGF signaling contributes to the Th2-mediated inflammatory response associated with *Schistosoma*-induced PH. We tested this hypothesis by concurrent pharmacologic blockade of the VEGFR, using the VEGFR/tyrosine kinase inhibitor SU5416, in mice also exposed to *S. mansoni* ova. We found that VEGFR blockade partially suppressed the Th2 inflammation in both the lung and the liver as well as the severity of pulmonary vascular remodeling, suggesting that VEGF signaling plays a pro-remodeling role in this model of the human disease.

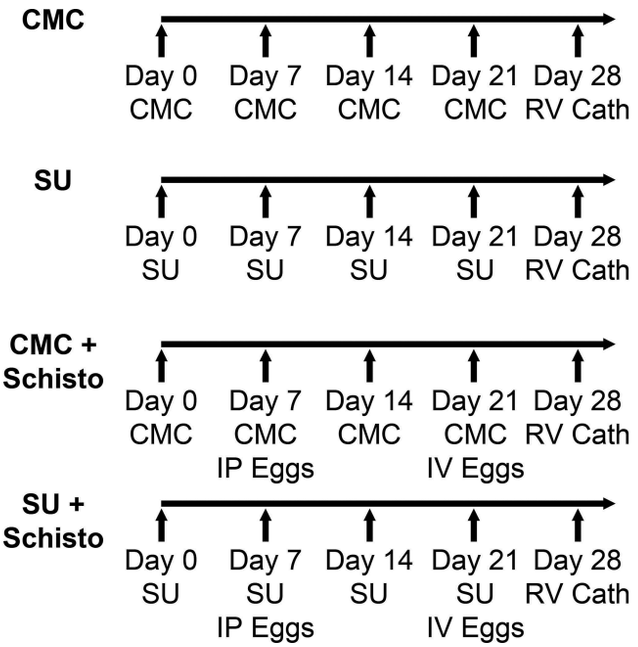

Figure 1. Schematic representation of the animal protocols used for *Schistosoma* ova (Schisto), SU5416 (SU), and carboxymethylcellulose (CMC) administration. SU5416 (20 mg/kg body weight) or CMC was administered subcutaneously weekly at the time points indicated. *Schistosoma*-exposed mice were intraperitoneally (IP) injected with eggs at a dose of 240 eggs/g body weight, followed 2 weeks later by intravenous (IV) injection of *Schistosoma mansoni* eggs at a dose of 240 eggs/g body weight. Hemodynamic measurements and tissue collection were performed on day 28. RV Cath: right ventricular catheterization.

METHODS

Animals

Wild-type C57Bl6/J mice were purchased from Taconic (Hudson, NY). All mice were housed under specific pathogen-free conditions in an American Association for the Accreditation of Laboratory Animal Care–approved facility. All experimental procedures in rodents were approved by the Animal Care and Use Committee. Data analyses were performed with coded experimental groups until reporting of the final data.

Treatments

Schistosoma mansoni eggs were obtained from homogenized and purified livers of Swiss-Webster mice infected with *S. mansoni* cercariae, provided by the Biomedical Research Institute (Rockville, MD). Experimental mice were intraperitoneally and intravenously challenged with *S. mansoni* eggs at the time points indicated in Figure 1, at a dose of 240 eggs/g body weight per administration. For cercarial infection, resulting in liver disease, 100 cercariae/mouse (collected from infected *Biomphalaria glabrata* snails) were placed in a vial, in which the mouse's tail was suspended for 30 minutes. SU5416 (Tocris Bioscience, Ellisville, MO) was reconstituted in dimethyl sulfoxide (DMSO), diluted into a working volume in carboxymethylcellulose (CMC), and administered at a dose of 20 mg/kg body weight, or the equivalent volume of DMSO/CMC alone, injected subcutaneously once weekly at the time points in Figures 1 and 7. Fasudil (LC Laboratories, Woburn, MA) was reconstituted in phosphate-buffered saline and administered intravenously at a dose of 30 mg/kg body weight during right ventricular catheterization after a stable pressure-volume loop was obtained; posttreatment pressures were recorded 5 minutes after fasudil administration.

Assessment of PH

Measurement of the right ventricular pressure was performed as previously described.[22] Briefly, the mice were anesthetized with ketamine/xylazine and ventilated through

Table 1. Reagents for immunostains on mouse tissue

Immunostain	Antigen retrieval	Block	Primary antibody	Secondary antibody	Tertiary reagent
Thrombomodulin (CD141)	Citrate buffer 30 min in steamer (Vector H-3300); rinses with TBST	10% horse serum in 1 : 1 5% BSA : Superblock (ScyTek AAA5000) 1 hr at RT	1 : 1,000 1 hr at RT (R&D Systems AF3894)	1 : 200 AF594 donkey anti-goat (Invitrogen A11058) 1 hr at RT	Vectashield with DAPI (Vector H-1200)
α–smooth muscle actin	Citrate buffer 30 min in steamer (Vector H-3300); rinses with TBST	Avidin 10 min, Biotin 10 min, mouse-on-mouse (MOM) kit blocking solution (Vector BMK-2202) 1 hr at RT	1 : 100 30 min at RT (Dako M0851)	MOM biotinylated anti-mouse reagent (Vector BMK-2202) 10 min at RT	Texas Red-streptavidin 1 : 2,000 (Invitrogen S872), Vectashield with DAPI (Vector H-1200)
PCNA	Citrate buffer 30 min in steamer (Vector H-3300); rinses with TBST	10% horse serum in 1 : 1 5% BSA/Superblock	1 : 50 1 hr at RT (Santa Cruz scbt 7907)	1 : 200 1 hr at RT AF488 donkey anti-rabbit (Invitrogen A21206)	Vectashield with DAPI (Vector H-1200)
IL-4	Citrate buffer 30 min in steamer (Vector H-3300); rinses with TBST	Peroxide block (Dako S2003) 10 min, 3% H_2O_2 in PBS 10 min, avidin 10 min, biotin 10 min, 10% goat serum in TBS 1 hr at RT	1 : 100 1 hr at RT (Abcam ab9622) in TBS	1 : 200 1 hr at RT biotinylated goat anti-rabbit (Vector BA5000) in TBS	SA-HRP 30 min at RT (Vector SA-5704), DAB (Vector SK-4100) 5 min at RT, hematoxylin 2 min at RT
IL-13	Citrate buffer 30 min in steamer (Vector H-3300); rinses with TBST	Peroxide block (Dako S2003) 10 min, 3% H_2O_2 in PBS 10 min, avidin 10 min, biotin 10 min, 10% rabbit serum in TBS	1 : 50 1 hr at RT (R&D Systems AF-213-NA) in TBS	1 : 200 1 hr at RT biotinylated rabbit anti-goat (Vector BA1000) in TBS	SA-HRP 30 min at RT (Vector SA-5704), DAB (Vector SK-4100) 5 min at RT, hematoxylin 2 min at RT
TUNEL	Manufacturer's instructions[a]	Manufacturer's instructions[a]	Manufacturer's instructions[a]	Manufacturer's instructions[a]	Manufacturer's instructions[a]

Note: TBST: Tris-buffered saline plus Tween; BSA: bovine serum albumin; RT: room temperature; DAPI: 4′,6-diamidino-2-phenylindole; PCNA: proliferating cell nuclear antigen; PBS: phosphate-buffered saline; TBS: Tris-buffered saline; SA-HRP: horseradish peroxidase streptavidin; DAB: diaminobenzadine; IL: interleukin; TUNEL: terminal deoxynucleotidyl transferase biotin-dUTP nick end labeling;

[a] Promega Dead End TUNEL Kit (catalog no. G3250).

a transtracheal catheter. The abdominal and thoracic cavities were opened, and a 1-Fr pressure-volume catheter (Millar PVR-1035, Millar Instruments, Houston, TX) was placed through the right ventricle apex to transduce the pressure. The blood was flushed out of the lungs, the right bronchus was sutured, and 2% agarose was instilled into the left lung through the transtracheal catheter. The left lung was removed, formalin fixed, and processed for paraffin embedding. The right lung was removed and divided into lobes, which were frozen. The right ventricle free wall was dissected from the heart and weighed relative to the septum and left ventricle (the Fulton index).

Histology and immunostaining

Lung and liver tissue was formalin fixed, paraffin embedded, and then sectioned and H&E (hematoxylin and eosin) stained. Immunostaining for α–smooth muscle actin (media), thrombomodulin (intima), TUNEL (terminal deoxynucleotidyl transferase biotin-dUTP nick end labeling; apoptosis), proliferating cell nuclear antigen (PCNA; proliferation), IL-4, and IL-13 was performed with the reagents listed in Table 1.

Protein assessment

A sample of the frozen right lung tissue was macerated and sonicated in radioimmunoprecipitation assay buffer (RIPA; Sigma R0278) containing antiproteases and antiphosphatases (Calbiochem 539131 and 524625, respectively), and protein concentration was determined by Bradford assay (BioRad 500-0006). The amount of protein was quantified by enzyme-linked immunosorbent assay (ELISA), using kits (IL-4: R&D Systems M4000B; IL-13: R&D Systems M1300CB; guanosine triphosphate [GTP]-RhoA: Cytoskeleton BK124), and normalized by total protein concentration.

Image analysis

Quantification of media and intima thickness in mouse lung tissue was determined as previously described.[13] Briefly, 10–15 images of vessels at 40× magnification were randomly acquired from masked paraffin-embedded samples stained for α–smooth muscle actin and thrombomodulin as described above. Image-processing software (Image Pro Plus, ver. 4.5.1, Media Cybernetics, Bethesda, MD) was used to identify the cross-sectional areas contained by the external perimeter of the media, the internal perimeter of the media, and the internal perimeter of the intima. The radius r_i for each of the three vessel layers i enclosing an area A_i was calculated with the equation $r_i = (|A_i/\pi|)^{1/2}$. The thicknesses of the media and intima were calculated as the differences between the respective radii and expressed as fractions of the external media radius.

Periegg granuloma volumes were measured with the optical rotator sterologic method.[23] Briefly, paraffin-embedded tissue was H&E stained, and 8–10 images of granulomas with a single visible ovum were acquired from each sample. The rotator method for object volume estimation was then applied with the ovum as the central reference point in the image-processing software (Image Pro Plus).

Statistics

The statistical analyses were performed in SigmaStat, version 2.03 (IBM, Armonk, NY). Data are presented as mean ± standard error. Differences between two groups

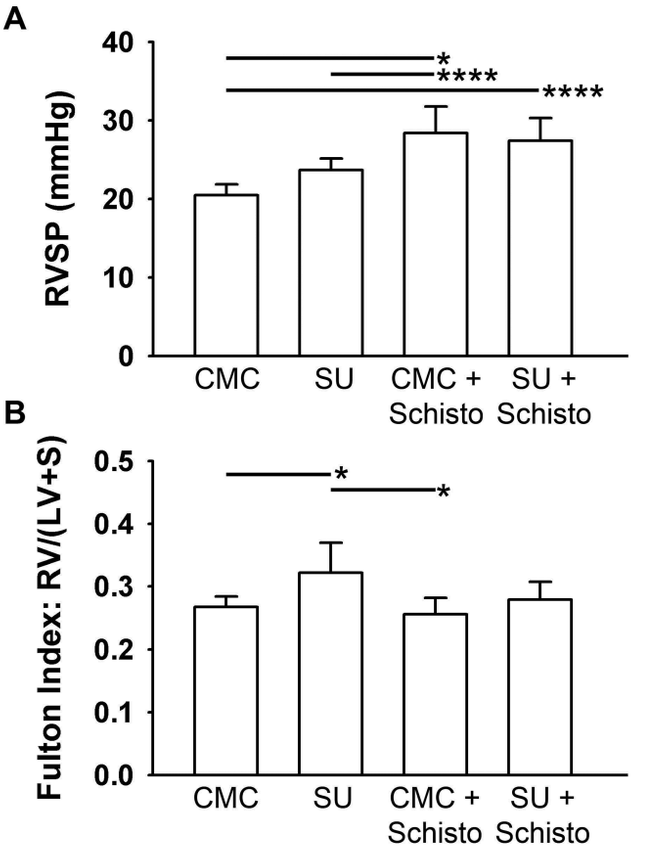

Figure 2. Effect of *Schistosoma* exposure (Schisto) and SU5416 (SU) treatment on right ventricular systolic blood pressure and right ventricular hypertrophy. *A*, Right ventricular systolic pressure (RVSP). *B*, Right ventricular hypertrophy (measured by Fulton index [ratio of right ventricle (RV) weight to the combined weight of the left ventricle (LV) and septum (S)]). $n = 5$–6 animals/group; ANOVA: $P < 0.001$ for RVSP, $P = 0.014$ for Fulton index. A single asterisk indicates $P < 0.05$ and 4 asterisks $P < 0.001$ by post hoc Tukey test. CMC: carboxymethylcellulose.

were assessed with Student's *t* test or the rank-sum test (for nonnormally distributed data). For comparison of three or more groups, analysis of variance or the Kruskal-Wallis test (for nonnormally distributed data) was used, followed by the Tukey post hoc test. In one instance, Grubb's test was used to identify an outlier ($P < 0.05$) and remove this point from statistical analysis; this point was in the non-*Schistosoma*-exposed, SU5416-treated group of the GTP-RhoA ELISA (Fig. 6*A*). All *P* values below 0.05 were considered to be statistically significant.

RESULTS

PH and pulmonary vascular remodeling were induced in mice with sequential challenge by intraperitoneal and intravenous *Schistosoma* eggs, which recapitulate the pulmonary effects of the natural infection.[13-15] Mice were ex-

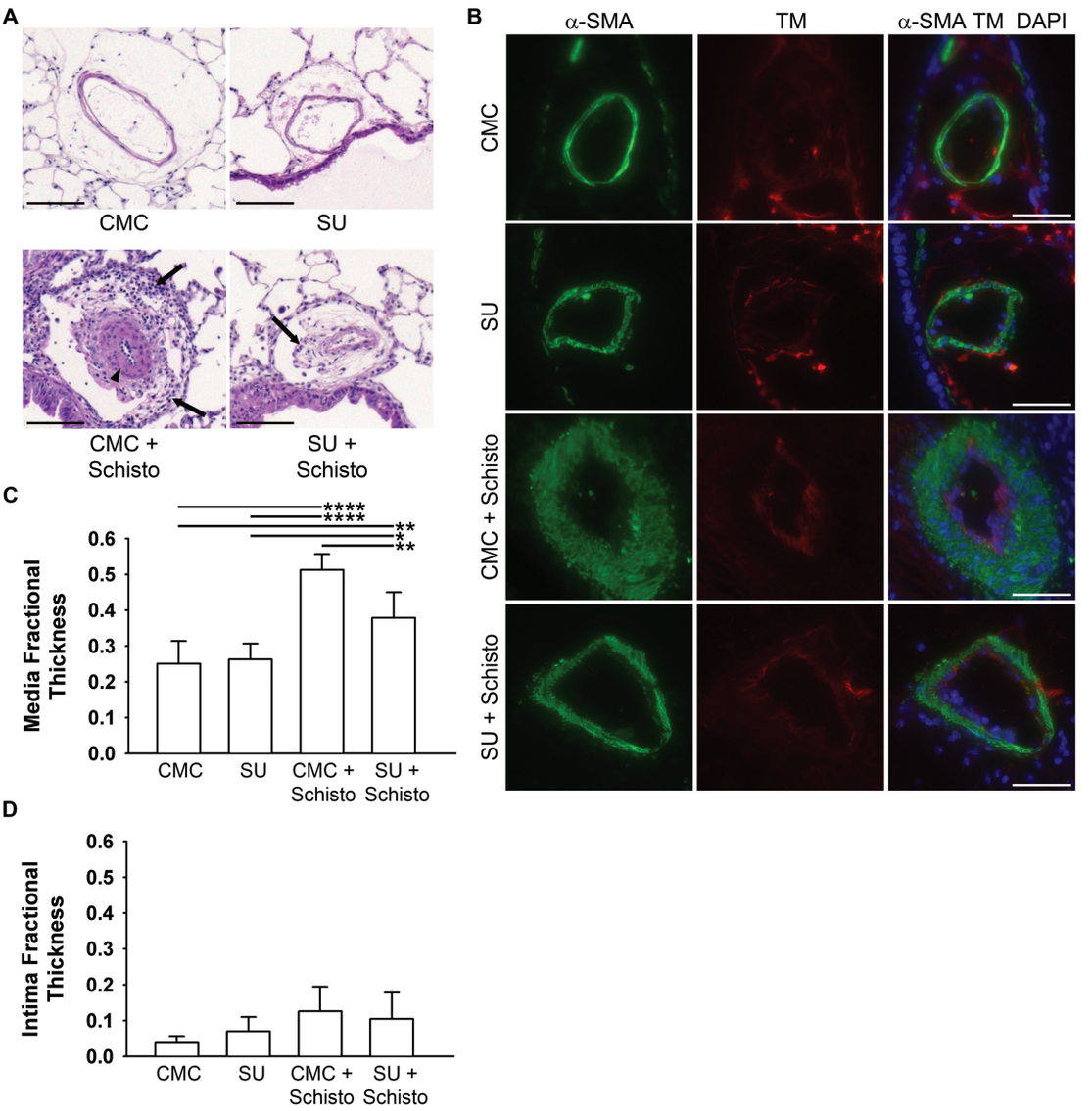

Figure 3. SU5416 attenuates vascular remodeling from *Schistosoma* exposure. *A*. Hematoxylin and eosin staining of representative samples (arrowhead: medial thickening; arrows: adventitial inflammatory cell infiltrates; scale bar: 100 μm). *B*, Immunofluorescence staining for α–smooth muscle actin (α-SMA; green: media) and thrombomodulin (TM; red: intima; blue: DAPI [4′,6-diamidino-2-phenylindole]; scale bars: 50 μm). *C*, *D*, Quantification of the media and intima layers. $n = 5$–6 animals/group; ANOVA: $P < 0.001$ for media, $P = 0.062$ for intima. A single asterisk indicates $P < 0.05$, a double asterisk $P < 0.01$, and 4 asterisks $P < 0.001$ by post hoc Tukey test. CMC: carboxymethylcellulose; SU: SU5416; Schisto: *Schistosoma*.

posed to four treatment strategies; we opted to precede *Schistosoma* egg challenge with VEGFR blockade to block a potential role for VEGF in triggering or contributing to the induced Th2 response (Fig. 1). The two groups intraperitoneally/intravenously exposed to *Schistosoma* eggs developed a significant increase in right ventricle systolic pressure (RVSP) when compared to control mice (Fig. 2*A*). Concurrent treatment with the VEGFR/tyrosine kinase inhibitor SU5416 (SU) did not significantly alter the RVSP, compared to *Schistosoma* exposure with CMC treatment. Mice treated with SU alone did not have a significant increase in RVSP but did develop significant right ventricle hypertrophy (Fig. 2*B*). *Schistosoma* exposure alone did not cause significant right ventricle hypertrophy, likely because of the relatively short experimental protocol (1 week after intravenous egg augmentation).

Histologic examination of the pulmonary vasculature by H&E staining revealed pulmonary arterial remodeling, characterized by medial thickening and adventitial inflammatory cell infiltrates, in the lungs of *Schistosoma*-exposed mice (Fig. 3*A*). The degree of medial thickening and the number of perivascular inflammatory cells were attenuated in *Schistosoma*-exposed mice that were concurrently treated with SU. To further characterize the vascular remodeling, immunostaining for α–smooth muscle actin (to localize the media) and thrombomodulin (to localize the intima) was performed (Fig. 3*B*). Quantification of the media and intima thickness revealed that both *Schistosoma*-

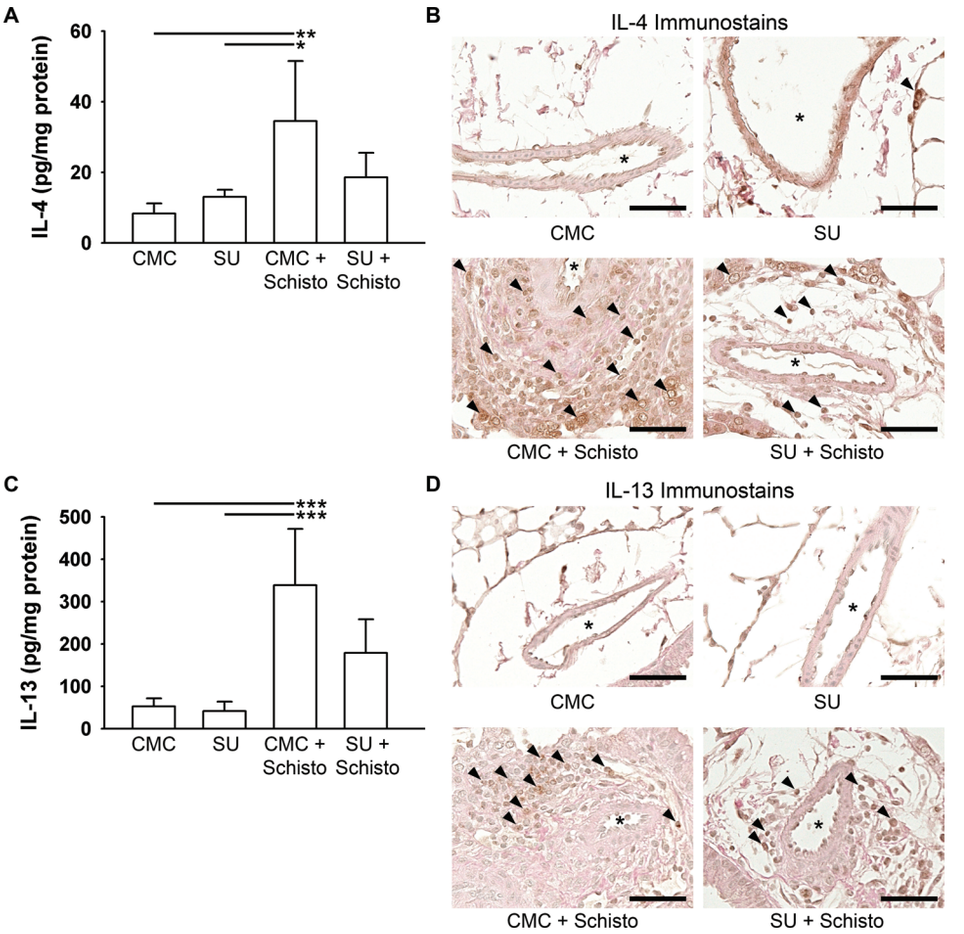

Figure 4. Interleukin (IL)-4 and IL-13 protein levels are increased in the lungs of *Schistosoma* (Schisto)-exposed mice and partially attenuated by concurrent SU5416 (SU) administration. *A*, Quantification of IL-4 protein levels, as measured by enzyme-linked immunosorbent assay (ELISA). $n = 4$ animals/group; ANOVA: $P = 0.014$; a single asterisk indicates $P < 0.05$ and a double asterisk $P < 0.01$ by post hoc Tukey test. *B*, Immunostain for IL-4 on representative lung sections from mice exposed to carboxymethylcellulose (CMC) or SU, with or without concurrent *Schistosoma* exposure (arrowheads: positively stained cells; asterisk: vessel lumen; scale bars: 50 μm). *C*, IL-13 protein levels, as measured by ELISA. $n = 4$ animals/group; ANOVA $P < 0.001$; 3 asterisks indicate $P < 0.005$ by post hoc Tukey test. *D*, Immunostain for IL-13 on representative lung sections from mice exposed to CMC or SU, with or without concurrent *Schistosoma* exposure (arrowheads: positively stained cells; asterisk: vessel lumen; scale bars: 100 μm).

exposed groups developed significant medial thickening, compared to mice not exposed to *Schistosoma* (Fig. 3*C*), and that concurrent treatment with SU significantly suppressed the medial thickening provoked by *Schistosoma* exposure. There were no significant differences in intimal thickness between any of the groups, although there was a trend toward increased intimal thickness with *Schistosoma* exposure ($P = 0.062$; Fig. 3*D*).

We next assessed the levels of the Th2 inflammatory cytokines IL-4 and IL-13 in whole-lung protein lysates (Fig. 4). The levels of both IL-4 and IL-13 were significantly increased by *Schistosoma* exposure, and there were trends toward decreases in these cytokines with concurrent SU treatment, consistent with a contributing role of VEGF in the Th2 cytokine profiles in this model (post hoc Tukey tests: $P = 0.13$ for IL-4, $P = 0.06$ for IL-13). The use of whole-lung lysate cytokine levels likely decreased the sensitivity of our analyses. Immunostaining for IL-4 and IL-13 demonstrated an increase in adventitial cells positively staining for both cytokines after *Schistosoma* expo-

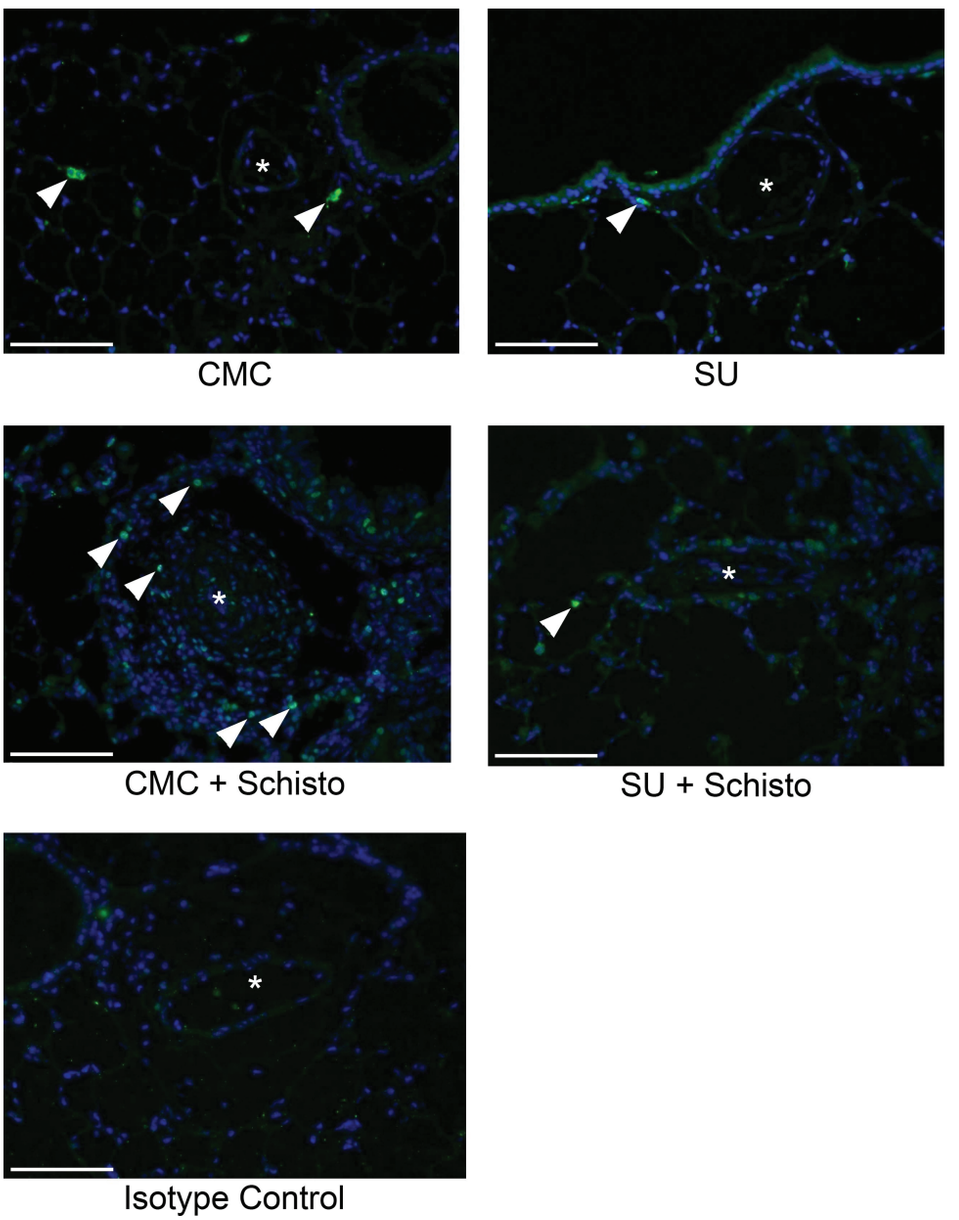

Figure 5. Adventitial cellular proliferation is increased in the lungs of *Schistosoma* (Schisto)-exposed mice and attenuated by concurrent SU5416 (SU) administration. Immunofluorescence staining for proliferating cell nuclear antigen (PCNA; green; arrowheads: PCNA-positive cells in the adventitia) and DAPI (4′,6-diamidino-2-phenylindole; blue; asterisk: vessel lumen). Scale bars: 100 μm. CMC: carboxymethylcellulose.

sure. With concurrent SU treatment, the density of the cells that stained positive for either IL-4 or IL-13 decreased. The inflammatory granuloma volumes in *Schistosoma* egg–exposed mice were not significantly different between the groups receiving CMC or SU in addition to *Schistosoma* exposure (data not shown).

We also sought to characterize cellular proliferation and apoptosis in the vasculature by immunostaining for PCNA and TUNEL. Vascular cell proliferation was largely absent in the media or intima of pulmonary arteries in all of the groups (Fig. 5). However, mice exposed to *S. mansoni* eggs had an increase in the number of adventitial PCNA-positive cells, which was suppressed by concurrent SU treatment. Significant apoptosis, as indicated by TUNEL staining, was not observed in the pulmonary arteries or perivascular regions in any of the groups (data not shown).

There is evidence that human schistosomiasis-associated PAH involves both pulmonary vasoconstriction and vascular remodeling.[24] We sought to determine the degree of vasoconstriction after SU treatment with or without concurrent *Schistosoma* egg exposure. We specifically interrogated the activity of the Rho kinase pathway, which we previously found to be a significant contributor in experimental PH induced by *Schistosoma* exposure[14] and has been implicated in pathologic vasoconstriction in other models of experimental PH.[25-27] We found a 2.6-fold increase ($P = 0.02$) in the concentration of activated (GTP-bound) RhoA in whole-lung lysates of concurrently SU-treated and *Schistosoma*-exposed mice, compared to mice treated with SU alone (Fig. 6*A*). Acute intravenous administration of fasudil, a Rho-associated coiled-coil containing protein kinase (ROCK) inhibitor, resulted in a minimal average decrease of 1.8 mmHg in the RVSP of mice treated with SU alone. However, fasudil administration in concurrently SU-treated and *Schistosoma*-exposed mice resulted in a significantly greater decrease in the RVSP, 4.0 mmHg ($P < 0.05$; Fig. 6*B*–6*D*).

We also sought to assess the VEGF-dependent cytokine response in another organ (the liver) that is affected by *Schistosoma* infection. We infected mice with *S. mansoni* cercariae and concurrently treated with CMC or SU (Fig. 7*A*), followed by quantification of IL-4 and IL-13 levels in whole-liver protein lysates. As in the lung, the levels of hepatic IL-4 and IL-13 were significantly increased by *Schistosoma* exposure (Fig. 7*B*, 7*C*). There was a trend toward a decrease in hepatic IL-4 with concurrent SU treatment (post hoc Tukey test: $P = 0.07$) but less so for IL-13 (nonparametric post hoc Dunn's test: $P = 0.20$). The inflammatory liver granuloma volumes in *Schistosoma* cercariae–infected mice were not significantly different between the groups receiving CMC or SU in addition to *Schistosoma* exposure (data not shown).

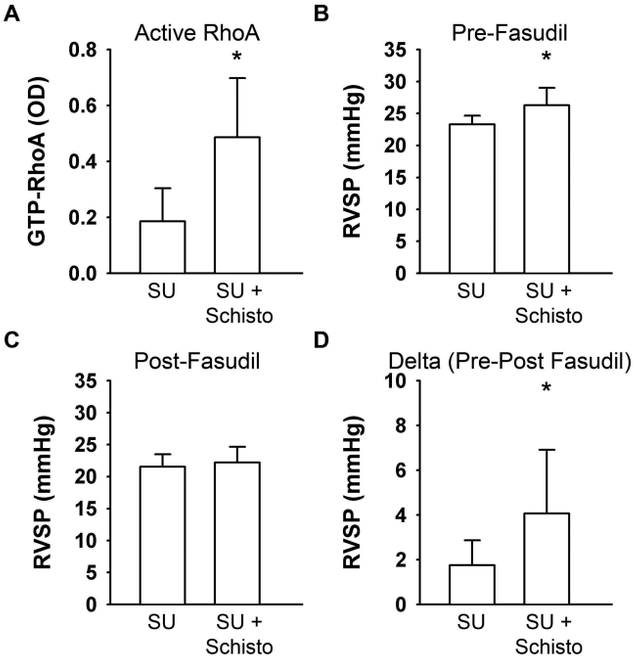

Figure 6. Rho kinase–mediated vasoconstriction is increased by *Schistosoma* (Schisto) exposure. *A*, Optical density (OD) of guanosine triphosphate (GTP)-bound (active) RhoA in whole-lung protein lysates; $n = 5$–6 animals/group; *t* test: $P = 0.02$. *B*–*D*, Right ventricular systolic pressure (RVSP) in SU5416 (SU)-treated mice with or without concurrent *Schistosoma* exposure recorded before (*B*) and 5 minutes after (*C*) fasduil administration and the decrease in pressure for each animal (*D*); $n = 8$–9 animals/group. In all panels, an asterisk indicates $P < 0.05$ by *t* test.

DISCUSSION

In this study, we present evidence that VEGF signaling is involved in the development of Th2 inflammation and vascular remodeling in the lungs of mice provoked by sensitization and intravenous exposure to *Schistosoma* ova, as evidenced by a decrease in Th2 inflammatory cytokines, perivascular inflammation, and pulmonary arterial medial thickening with concurrent pharmacological blockade of the VEGFRs VEGFR1 and VEGFR2. Our findings are consistent with previous studies suggesting that VEGF is a positive regulator of inflammation in the lung.[7-9] We have previously shown that there are both bone marrow–derived and locally proliferating cells in the vasculature of *Schistosoma*-exposed mice.[14] The mechanism by which VEGF upregulates pulmonary inflammation, and thereby promotes PH, in the mouse may be due to increasing inflammatory cell recruitment or localized proliferation,

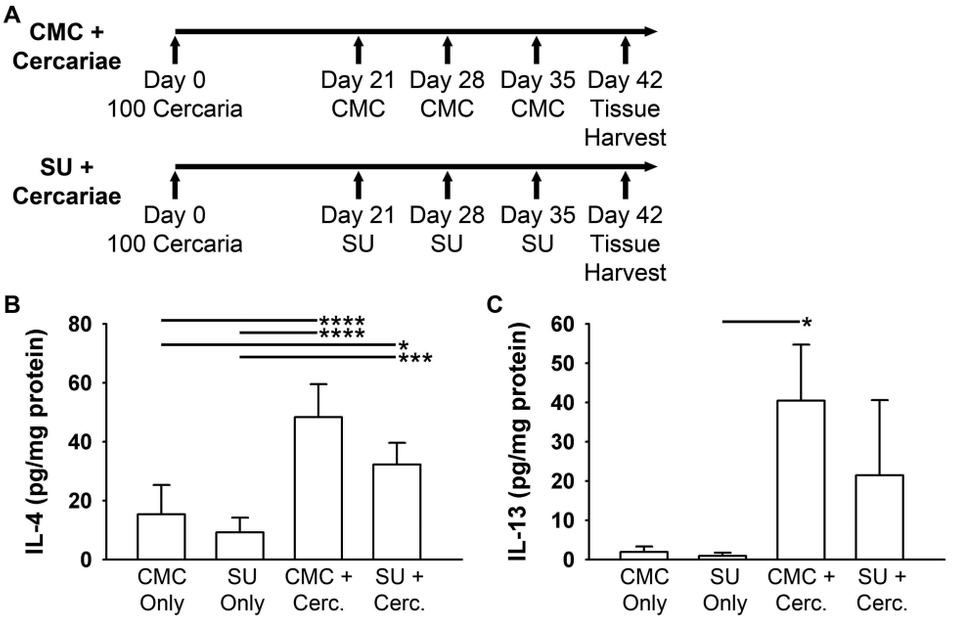

Figure 7. Interleukin (IL)-4 and IL-13 protein levels are increased in the livers of *Schistosoma*-infected mice and attenuated by concurrent SU5416 administration. *A*, Schematic representation of the animal protocols used for SU5416 (SU; 0 mg/kg) or carboxymethylcellulose (CMC) administration and *Schistosoma* cercariae (Cerc.) infection. *B*, Quantification of IL-4 protein levels, as measured by enzyme-linked immunosorbent assay (ELISA). *C*, IL-13 protein levels, as measured by ELISA. $n = 4–6$ animals/group; ANOVA: $P < 0.001$ for IL-4; ANOVA on ranks: $P = 0.006$ for IL-13. A single asterisk indicates $P < 0.05$, 3 asterisks $P < 0.005$, and 4 asterisks $P < 0.001$ by post hoc Tukey test (*B*) or post hoc Dunn's test (*C*).

because SU treatment decreases adventitial inflammatory cell density after either *Schistosoma* or inhaled ovalbumin exposures.[7] We furthermore extended these studies by finding that VEGF is also a partial regulator of Th2 inflammation in the liver.

There have been conflicting reports regarding the role of VEGF signaling in experimental animal models of inflammation-driven pulmonary vascular disease. In the mouse, VEGF overexpression has been shown to promote Th2 inflammation,[7] which in turn can result in pulmonary vascular disease.[6,16-20] Conversely, in the rat, VEGFR blockade has been shown to exacerbate pulmonary vascular disease due to antigen-induced Th2 inflammation, resulting in PH.[11] In the mouse, however, although antigen-induced Th2 inflammation in the lung suffices to cause pulmonary arterial muscularization,[6] VEGFR blockade does not exacerbate this phenotype, although when combined with hypoxia it may contribute to the development of PH, as it does in the rat.[12,28]

Numerous studies have documented additional differences between the pulmonary vascular responses of mice and rats (many of which are discussed in a recent review of mouse models of PAH[29]), and it is far from clear whether any one model is more relevant to the human disease than any other model. For example, the severity of hypoxia-induced PH and vascular remodeling is significantly less in mice than in rats,[30] and hypoxia induces different gene expression patterns in the lungs of mice and in the lungs of rats.[31] The difference between our finding of protection from Th2-induced inflammation and vascular remodeling in mice with *Schistosoma* exposure and SU treatment, as compared to worsened disease with ovalbumin exposure and SU in the rat,[11] provides another example of species-specific differences in experimental models of PH. While the model phenotypes could also be explained by differences in the specific inflammatory stimuli (ovalbumin vs. *Schistosoma* ova), the fact that ovalbumin exposure also does not synergize with SU in the mouse[12] suggests that there are key differences between Th2-stimulated vascular disease in rats and that in mice. One potential factor may be the more extensive bronchiolar blood supply in rats compared to that in mice, providing a route of entry for immune cell populations.[32,33]

PH results from a combination of fixed vascular remodeling and vasoconstriction. We tested the role of Rho-mediated vasoconstriction in *Schistosoma*-induced PH with concurrent SU treatment; Rho-mediated vasoconstriction has been shown to be implicated in pathologic vasoconstriction in *Schistosoma*-induced and other models of experimental PH and is an area of active clinical investiga-

tion.[14,25-27,34,35] VEGFR blockade alone did not result in significant ROCK-mediated vasoconstriction, while the levels of activated RhoA and ROCK-mediated vasoconstriction were increased with concurrent *Schistosoma* exposure. The decrease in RVSP induced by fasudil in the SU-*Schistosoma* group is comparable to the decrease in RVSP induced by fasudil we previously observed in *Schistosoma*-alone mice (6.9 ± 3.4 mmHg).[14] Of note, some patients with *Schistosoma*-induced pulmonary vascular disease have a significant component of vasoconstriction.[24]

In summary, we found that VEGF signaling is necessary for the immune-stimulated vascular remodeling induced by *Schistosoma* egg exposure in the mouse. Further studies are needed to clarify the role of VEGF and the potential therapeutic opportunity of blocking or augmenting VEGF signaling in patients with PAH in general and *Schistosoma*-induced PAH specifically.

ACKNOWLEDGMENTS

Schistosoma-infected mice were provided by the Biomedical Research Institute via the National Institute of Allergy and Infectious Diseases (NIAID) schistosomiasis resource center under National Institutes of Health (NIH)-NIAID contract HHSN272201000005I. These materials can be obtained by contacting the Biodefense and Emerging Infections Research Resources Repository (BEI Resources).

Source of Support: NIH grant K08HL105536 (BBG), Parker B. Francis fellowship (BBG), American Recovery and Reinvestment Act grant RC1HL100849 (RMT), and Cardiovascular Medical Research and Education Fund (RMT).

Conflict of Interest: None declared.

REFERENCES

1. Rabinovitch M. Autoimmune disease and unexplained pulmonary hypertension. Circulation 1992;85(1):380–381.
2. Mouthon L, Guillevin L, Humbert M. Pulmonary arterial hypertension: an autoimmune disease? Eur Respir J 2005;26(6):986–988.
3. Nicolls MR, Taraseviciene-Stewart L, Rai PR, Badesch DB, Voelkel NF. Autoimmunity and pulmonary hypertension: a perspective. Eur Respir J 2005;26(6):1110–1118.
4. Tuder RM, Voelkel NF. Pulmonary hypertension and inflammation. J Lab Clin Med 1998;132(1):16–24.
5. Hecker M, Zaslona Z, Kwapiszewska G, Niess G, Zakrzewicz A, Hergenreider E, Wilhelm J, et al. Dysregulation of the IL-13 receptor system: a novel pathomechanism in pulmonary arterial hypertension. Am J Respir Crit Care Med 2010;182(6):805–818.
6. Daley E, Emson C, Guignabert C, de Waal Malefyt R, Louten J, Kurup VP, Hogaboam C, et al. Pulmonary arterial remodeling induced by a Th2 immune response. J Exp Med 2008;205(2):361–372.
7. Lee CG, Link H, Baluk P, Homer RJ, Chapoval S, Bhandari V, Kang MJ, et al. Vascular endothelial growth factor (VEGF) induces remodeling and enhances T_H2-mediated sensitization and inflammation in the lung. Nat Med 2004;10(10):1095–1103.
8. Lee YC, Kwak YG, Song CH. Contribution of vascular endothelial growth factor to airway hyperresponsiveness and inflammation in a murine model of toluene diisocyanate-induced asthma. J Immunol 2002;168(7):3595–3600.
9. Corne J, Chupp G, Lee CG, Homer RJ, Zhu Z, Chen Q, Ma B, et al. IL-13 stimulates vascular endothelial cell growth factor and protects against hyperoxic acute lung injury. J Clin Invest 2000;106(6):783–791.
10. Taraseviciene-Stewart L, Kasahara Y, Alger L, Hirth P, McMahon G, Waltenberger J, Voelkel NF, Tuder RM. Inhibition of the VEGF receptor 2 combined with chronic hypoxia causes cell death-dependent pulmonary endothelial cell proliferation and severe pulmonary hypertension. FASEB J 2001;15(2):427–438.
11. Mizuno S, Farkas L, Al Husseini A, Farkas D, Gomez-Arroyo J, Kraskauskas D, Nicolls MR, Cool CD, Bogaard HJ, Voelkel NF. Severe pulmonary arterial hypertension induced by SU5416 and ovalbumin immunization. Am J Respir Cell Mol Biol 2012;47(5):679–687.
12. Nicolls MR, Mizuno S, Taraseviciene-Stewart L, Farkas L, Drake JI, Al Husseini A, Gomez-Arroyo JG, Voelkel NF, Bogaard HJ. New models of pulmonary hypertension based on VEGF receptor blockade-induced endothelial cell apoptosis. Pulm Circ 2012;2(4):434–442.
13. Graham BB, Mentink-Kane MM, El-Haddad H, Purnell S, Zhang L, Zaiman A, Redente EF, et al. Schistosomiasis-induced experimental pulmonary hypertension: role of interleukin-13 signaling. Am J Pathol 2010;177(3):1549–1561.
14. Graham BB, Chabon J, Gebreab L, Poole J, Debella E, Davis L, Tanaka T, et al. Transforming growth factor-β signaling promotes pulmonary hypertension caused by *Schistosoma mansoni*. Circulation 2013;128(12):1354–1364.
15. Graham BB, Chabon J, Kumar R, Kolosionek E, Gebreab L, Debella E, Edwards M, et al. Protective role of IL-6 in vascular remodeling in *Schistosoma* pulmonary hypertension. Am J Respir Cell Mol Biol 2013;49(6):951–959.
16. Chitsulo L, Loverde P, Engels D. Schistosomiasis. Nat Rev Microbiol 2004;2(1):12–13.
17. de Cleva R, Herman P, Pugliese V, Zilberstein B, Saad WA, Rodrigues JJ, Laudanna AA. Prevalence of pulmonary hypertension in patients with hepatosplenic Mansonic schistosomiasis–prospective study. Hepato-gastroenterology 2003;50(54):2028–2030.
18. Graham BB, Bandeira AP, Morrell NW, Butrous G, Tuder RM. Schistosomiasis-associated pulmonary hypertension. Chest 2010;137(6 suppl.):20S–29S.
19. Lapa M, Dias B, Jardim C, Fernandes CJC, Dourado PMM, Figueiredo M, Farias A, et al. Cardiopulmonary manifestations of hepatosplenic schistosomiasis. Circulation 2009;119(11):1518–1523.
20. Ward TJC, Fenwick A, Butrous G. The prevalence of pulmonary hypertension in schistosomiasis: a systematic review. PVRI Rev 2011;3(1):12–21.
21. Bryan BA, Dennstedt E, Mitchell DC, Walshe TE, Noma K, Loureiro R, Saint-Geniez M, Campaigniac J-P, Liao JK, D'Amore PA. RhoA/ROCK signaling is essential for multi-

ple aspects of VEGF-mediated angiogenesis. FASEB J 2010; 24(9):3186–3195.
22. Hemnes AR, Forfia PR, Champion HC. Assessment of pulmonary vasculature and right heart by invasive haemodynamics and echocardiography. Int J Clin Pract Suppl 2009; (162):4–19.
23. Tandrup T, Gundersen HJ, Jensen EBV. The optical rotator. J Microsc 1997;186(2):108–120.
24. Japyassu FA, Mendes AA, Bandeira AP, Oliveira FR, Sobral FD. Hemodynamic profile of severity at pulmonary vasoreactivity test in schistosomiasis patients. Arq Bras Cardiol 2012;99(3):789–796.
25. Oka M, Homma N, Taraseviciene-Stewart L, Morris KG, Kraskauskas D, Burns N, Voelkel NF, McMurtry IF. Rho kinase-mediated vasoconstriction is important in severe occlusive pulmonary arterial hypertension in rats. Circ Res 2007;100(6):923–929.
26. Nagaoka T, Morio Y, Casanova N, Bauer N, Gebb S, McMurtry I, Oka M. Rho/Rho kinase signaling mediates increased basal pulmonary vascular tone in chronically hypoxic rats. Am J Physiol Lung Cell Mol Physiol 2004;287(4): L665–L672.
27. Nagaoka T, Fagan KA, Gebb SA, Morris KG, Suzuki T, Shimokawa H, McMurtry IF, Oka M. Inhaled Rho kinase inhibitors are potent and selective vasodilators in rat pulmonary hypertension. Am J Respir Crit Care Med 2005;171 (5):494–499.
28. Ciuclan L, Bonneau O, Hussey M, Duggan N, Holmes AM, Good R, Stringer R, et al. A novel murine model of severe pulmonary arterial hypertension. Am J Respir Crit Care Med 2011;184(10):1171–1182.
29. Gomez-Arroyo J, Saleem SJ, Mizuno S, Syed AA, Bogaard HJ, Abbate A, Taraseviciene-Stewart L, et al. A brief overview of mouse models of pulmonary arterial hypertension: problems and prospects. Am J Physiol Lung Cell Mol Physiol 2012;302(10):L977–L991.
30. Voelkel NF, Tuder RM, Wade K, Höper M, Lepley RA, Goulet JL, Koller BH, Fitzpatrick F. Inhibition of 5-lipoxygenase-activating protein (FLAP) reduces pulmonary vascular reactivity and pulmonary hypertension in hypoxic rats. J Clin Invest 1996;97(11):2491–2498.
31. Hoshikawa Y, Nana-Sinkam P, Moore MD, Sotto-Santiago S, Phang T, Keith RL, Morris KG, et al. Hypoxia induces different genes in the lungs of rats compared with mice. Physiol Genomics 2003;12(3):209–219.
32. Crossno JT Jr., Garat CV, Reusch JE, Morris KG, Dempsey EC, McMurtry IF, Stenmark KR, Klemm DJ. Rosiglitazone attenuates hypoxia-induced pulmonary arterial remodeling. Am J Physiol Lung Cell Mol Physiol 2007;292(4):L885–L897.
33. Stenmark KR, Meyrick B, Galie N, Mooi WJ, McMurtry IF. Animal models of pulmonary arterial hypertension: the hope for etiological discovery and pharmacological cure. Am J Physiol Lung Cell Mol Physiol 2009;297(6):L1013–L1032.
34. Fukumoto Y, Yamada N, Matsubara H, Mizoguchi M, Uchino K, Yao A, Kihara Y, et al. Double-blind, placebo-controlled clinical trial with a rho-kinase inhibitor in pulmonary arterial hypertension. Circ J 2013;77(10):2619–2625.
35. Toba M, Alzoubi A, O'Neill KD, Gairhe S, Matsumoto Y, Oshima K, Abe K, Oka M, McMurtry IF. Temporal hemodynamic and histological progression in Sugen5416/hypoxia/normoxia-exposed pulmonary arterial hypertensive rats. Am J Physiol Heart Circ Physiol 2014;306(2):H243–H250.